Are fungus-growing termites super sediment-sorting insects of subtropical environments?

John Van Thuyne [a,b,*], Isacco Darini [a], Ali Mainga [b], Eric P. Verrecchia [a]

[a] *Institute of Earth Surface Dynamics, Lausanne University, 1015, Lausanne, Switzerland*
[b] *Van Thuyne-Ridge Research Center, PO 115, Maun, Botswana*

ABSTRACT

Fungus-growing termites have long been considered as ecosystem engineers for the modifications they make to the soil, through their ability to concentrate nutrients and create patches of fertile land. However, few studies have highlighted the degree to which, in building their mounds, they are able to modify the grain-size distributions of the sediments and soils in their surroundings. Therefore, the aim of this study is to document the potential impact of fungus-growing termites on sediment sorting of their environment. The assessment is based on comparisons between two different mounds and their associated control soils developed in contrasting grain-size settings, one on sand and the other on fine material (diatomite). The sedimentary modifications carried out by termites between these two parent materials and associated constructed mounds are addressed using techniques mostly based on grain-size distributions (performed with End-Member Mixing Analyses) and soil micromorphology. In order to conduct this investigation, two fungus-growing termites' mounds were selected in the Chobe Enclave District, northern Botswana. The key questions of this study center on the capacity of fungus-growing termites to (i) adapt to any kind of parent material to build their mounds, and (ii) enrich or deplete this parent soil to meet their texture requirements in terms of mound stability and other mechanical properties to insure the success of the colony. This study demonstrated that fungus-growing termites assemble the mandatory texture required for the functions and properties of their mounds, whatever a given parent material, by selecting, transporting, and mixing the various grain sizes. To conclude, the sorting by fungus-growing termites must be considered when reconstructing paleoenvironment based on particle-size distributions.

1. Introduction

Fungus-growing termites have long been considered as ecosystem engineers (Jones, 1990) for the modifications they bring to the soil, their ability to concentrate nutrients, and their capacity to create patches of fertile land. They are also considered as the predominant decomposer organisms in dry savannas, where they are responsible for around 20% of all organic carbon mineralization (Aanen and Eggleton, 2005). In addition, their mounds have the potential to retain water for long periods of time (Turner, 2006). Although fungus-growing termites have obvious specific capabilities to change their environment, only a few studies have highlighted their ability to modify the grain-size distributions of sediments and soils that form the environment where they develop (Jouquet et al., 2002). In the area of this study, there are mainly sands, but there are also some concentrations of fine material, offering the opportunity to compare the impact of fungus-growing termites on

two different and contrasting grain-size settings. The sedimentary modifications carried out by termites between these two parent materials and the constructed mounds are assessed using techniques mostly based on grain-size distributions and soil micromorphology. Indeed, only a few studies have combined both methods to highlight the role fungus-growing termites play in the selection of grain sizes to build their epigeal mounds (Abe et al., 2009). In order to conduct this investigation, two fungus-growing termites' mounds were selected in the Chobe Enclave District, northern Botswana, in the surroundings of the Van Thuyne Ridge (VTR) Research Center (Fig. 1). The approach developed in this study focuses on textures and micromorphological patterns of mounds built by fungus-growing termites of the Macrotermitinae sub-family, compared to control soils and sediments in the vicinity, which are considered undisturbed by termites. Knowing that these mounds will be dismantled by rain, gravity, and bioturbation with time, it is obvious that some modifications in textures and patterns resulting

---

from termite direct activity will only remain partially intact in the soil through time.

Control sediments, not affected by termites, and their two associated fungus-growing termites mounds, are situated in a subtropical semiarid region of northeast Botswana. They are at the same altitude, in the same geomorphological settings (floodplains), at only 2 km from each other (Fig. 1) and are subject to the same weather conditions.

Therefore, the key questions of this study center on the capacity of fungus-growing termites (i) to adapt to any kind of parent material to build their mounds, (ii) and to enrich or deplete this parent soil to meet their texture requirements in terms of mound stability and appropriate settings to insure the success of the colony. Indeed, the texture of their respective construction should converge to a required optimum by selecting, transporting, and mixing at will the various grain sizes at disposition from the surrounding environment.

2. Materials and methods

2.1. Geomorphological settings of the termitaria

The Chobe Enclave District – The Chobe Enclave District is located in the northeastern part of Botswana (Fig. 1A), bordered in the southeast by the Chobe Forest Reserve, in the south by the Chobe National Park, and in the northwest by the Linyanti River; it is approximately 30 km wide (N–S) and 60 km long (E-W), totalling 1690 km^2 (Jones, 2002). It is

situated at a latitude of 20° S in a subtropical zone with a semiarid climate of the type BSh (Beck et al., 2018, Fig. 1B). Rainfalls are concentrated from November to March, with an average of 600 mm, and the evapotranspiration is estimated at 1800 mm per year. A yearly flood occurs during the dry season in June and July, with high waters flowing from the Kwando catchment area in Angola, as well as the Zambezi River, creating a back flow up the Chobe river into the Chobe Enclave District. The entire area is physically bordered to the northwest by the Linyanti fault and to the southeast by the Chobe fault, both belonging to the Okavango Rift Zone (ORZ) and probably related to the East-African Rift (Kinabo et al., 2008). These tectonic settings form a 80 km north-south oriented graben, which is extremely flat with a slight tilt (0.01%) toward the south-east. The entire region is nearly devoid of human beings (population/km^2 = 2), but includes a rich diversity and a very high density of wildlife (e.g. approximately 8000 elephants; Jones 2002).

Geological setting – The study area is located in the Kalahari basin, a continuous sand body of 2.5 million km^2. The Ghanzi-Chobe basin in northern Botswana consists of a linear belt of volcano-sediments that were deposited during Meso-Neoproterozoic times following extension tectonics (Modisi et al., 2000). The Karoo bedrock i.e. Karoo Supergroup is a widespread stratigraphic unit south of the Kalahari Desert consisting of a sequence of siliciclastic sediments deposited between the late carboniferous and early Jurassic. On top lies the Kalahari group with sediment thickness going up to 300 m. In the Chobe Enclave, the
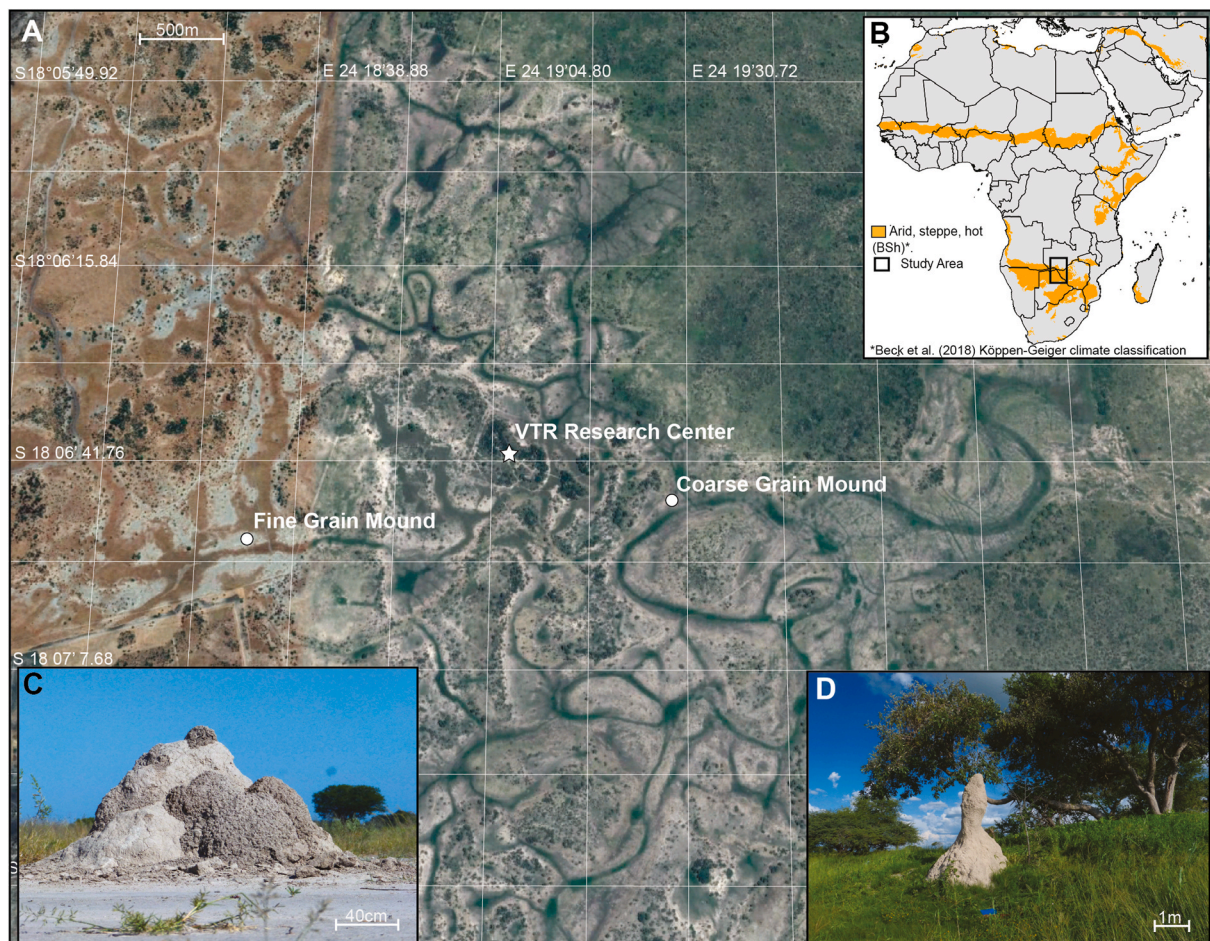

Fig. 1:. Geographical settings. (A) General view of the study area in the Chobe Enclave District (northern Botswana), comprised of a large floodplain with dambo and river channels; coarse and fine grain mounds are indicated. VTR: Van Thuyne-Ridge Research Center. (B) Map of Africa showing the BSh climate distribution, i.e. "*arid steppe hot*" from Beck et al. (2018); the black rectangle indicates the study area. (C) View of the fine grain termite mound. The two different grey colours indicate two different stages of mound building. (D) View of the coarse grain termite mound emerging from dambo grass. (For interpretation of the references to color in this figure legend, the reader is referred to the Web version of this article.)

Kalahari Sands (KS) deposits compose the substratum. The origin of these unconsolidated Kalahari Sands is still poorly understood and remains controversial (Thomas and Shaw, 1991). Nevertheless, their origin is principally attributed to in situ weathering of the subsurface Karoo bedrock (Baillieul, 1975). In addition, as suggested by Bull (1981), aeolian processes remain of great importance in the region's environmental history as means of KS reworking. The depth of KS can reach 800 m in the southern part of the Kalahari Basin. These sands are largely composed of quartz grains, i.e. 90% or more by weight (Thomas and Shaw, 1991). The KS are extremely well sorted (Humphries and Mc Carthy, 2014), a property emphasized by their leptokurtic curves. The KS have been characterized by various authors and fall into narrow grain-size distribution classes (Table 1). Within these deposits, a variety of soils developed (e.g. Chernozems, kastanozems, Solonchaks), the predominant one being the arenosols type (Romanens et al., 2019). Alluvial white sands cover floodplain and infill paleochannels. Carbonate and diatomite beds were found outcropping in the central part of the Enclave. They are thought to be ancient palustrine/lacustrine deposits formed during the Quaternary wet periods (Burrough and Thomas 2008). The endorheic nature of the basin led to aeolian, fluvial and/or lacustrine sediment accumulation since the Cretaceous (Grove, 1969).

Dust and desert loess – Airborne dust and desert loess have been traced back to the adjacent Kalahari sand sea (Crouvi et al., 2010), where they were picked up and transported by the predominant southern hemisphere winds. Two meteorological processes are at work: (i) a counter-clockwise subtropical semi-permanent continental anticyclone centred above the Kalahari high pressure cell, which is more intense during winter and weaker in summer (Landman et al., 2001), and (ii) the easterly trade winds. Both mechanisms collect and transport the fine fractions of the KS and move them in an anticlockwise direction redistributing these loess and dusts throughout the Kalahari Basin. Desert loess includes the desert loess *per se* and the airborne dust (Crouvi et al., 2010). First, in order to be considered as a true desert loess, sediments must satisfy certain criteria, i.e. (i) they must be distant from any past or present glaciated regions, (ii) they should not be more than 300 km away from the source, (iii) mineral compositions of the source and the coarse silt fraction of the loess should be similar, and (iv) the source should be located upwind (Crouvi et al., 2010). Loess are also defined by their grain sizes ranging from clay to very fine sand: the dominant fraction is coarse silt (20–63 μm), possibly extending into the finest sand fractions, the median grain size ranging from 50 to 80 μm, depending on the sources (Crouvi et al., 2010). Large quantities of material circulate in the anticyclonic system over southern Africa with an estimated 11.5 million tons of material transported annually across the Okavango region (Tyson et al., 1996). The Makgadikgadi pans, situated approximately 250 km south of the studied area, have been identified as one of the principle dust sources of southern Africa (Prospero et al., 2002), but further sand seas, such as the Kalahari (250 km) and its pans, are also considered to be important contributors of desert loess (Thomas and Shaw, 1991). The dust and loess of the region are composed of fine-grained material, which is usually poorly sorted with an average grain size between 30 and 60 μm (Humphries and Mc Carthy, 2014). All local and regional geomorphological features, such as channels, pans, burned vegetation, peat fires, floodplains, sand dunes, sand lakes, and

islands, are the other possible contributors to this dust. This airborne material consists of fine-grained quartz and amorphous silica associated with clay minerals, especially kaolinite (Humphries and Mc Carthy, 2014). Consequently, origins of dust and desert loess in the Chobe Enclave District are considered to be either local, i.e. coming from proximate geomorphological features <30 km distant, or regional.

Diatomite mud – Today, diatoms are extremely common in the rivers surrounding the Okavango Delta, but they have also formed large deposits in the past. Their sizes vary greatly from 3 μm to 500 μm, but the species encountered in the study area are generally very small, i.e. between 10 μm and 20 μm, 30 μm for the largest. More than 180 species have been documented in the Okavango Delta (Cholnoky, 1966). Moreover, during the past, their accumulation as fossilized remains produced large deposits of diatomaceous earth. These diatomaceous earths were mostly formed during sedimentation in stagnant water under neutral to slightly alkaline conditions and are found in ancient lake beds and on the lee side of sand ridges and shorelines (Thomas and Shaw, 1991).

Termitaria environment and control sediments – Both termitiaria are close to the VTR Research Center (GPS coordinates: 18°06′41″ south, 24°19′04″ east; Fig. 1A and B). The average depth of the water table in the area is approximately 26 m.

The termitarium built on fine silty parent material (Fig. 1C) is located on a flat open dry floodplain with little grass cover, where rainwater can collect and remain for a variable period of time each year. Occasionally, there is a flood. The area is defined as a *Combretum* woodland, the dominant species being *Combretum hereroense*, with some *Acacia nigrescens*. The two 80 cm deep trenches of the control sediments, at a distance of 20 m and 40 m from the mound, respectively, were dug in a fine grain diatomitic sediment. Rainwater does not penetrate easily due to the high silt and clay contents. Instead, runoff water evaporates easily directly from the surface. The pH_{H2O} of the control soil is situated at 6.5.

The termitarium built on a sandy parent material (Fig. 1D) is part of an alignment of termite mounds situated along a channel. This mound is situated on a fluvial terrace, at the edges of an occasional floodplain, where rainwater can accumulate during the rainy season. A low slope connects the termite mound site to the present-day floodplain. The area is covered by a dry grassland growing on top of a sandy alluvial deposit. The two main types of grasses present are *Aristida meridionalis* and *Bulbostylis hispidula* (Vittoz et al., 2020). The two control sediment trenches are at a distance of 20 m and 40 m from the mound, respectively, and are 80 cm deep. Their texture corresponds to a sand, with a very low silt-clay content. The pH_{H2O} of the control soil is situated at 7.6.

Why choose only two termitaria? – As observed by Mermut et al. (1984), if the environmental conditions are similar, construction types within the same species, and even between species, will remain alike. However, if the environmental conditions are different, even within the same species, construction types can vary. Davies et al. (2016) noted that the geological substratum does not seem to influence the type of construction within the same species or between species. Pomeroy (1978) spotted the occurrence of the same mound types on several different soils as evidence of a strong genetic component in the determination of mound structure. This is why it was preferable to choose similar environmental conditions for the two mounds, but with two distinctive substrata in order to observe the variations in the selection of grain sizes by the termites. In addition, according to Darlington and Dransfield (1987) and Turner (2006), no variability in the construction process is observed between the first and last stages of the building of a termitarium: it is only a repetitive function, which starts small and ends up big, thus choosing a medium termitarium of a few years and a small termitarium of a couple of years old does not imply any structural variations. Finally, as *Macrotermes michaelseni* (which belongs to the fungus-growing sub-family of Macrotermitinae) thrive and are the dominant species in the Chobe, it is reasonable to conceive that this environment is optimal for them (Korb and Linsenmair, 1998). Consequently, as Jouquet et al. (2016) demonstrated, when an environment is

Table 1
Average grain sizes of the Kalahari sands from various locations and references.

Location	Average size	Author
Kalahari dune field	125–220 μm	Cook (1980)
Namib sand sea	200 μm	Lancaster (1981)
Kalahari dune crest	175 μm	Watson (1986)
Southwest Kalahari	190–240 μm	Lancaster (1986)
Central Kalahari (Ghanzi)	170–225 μm	Wang et al. (2007)
Central Kalahari (Tshane)	210–230 μm	Wang et al. (2007)
Northern Botswana	200 μm	Thomas and Shaw (1991)
Namib sand sea	170–340 μm	Crouvi et al. (2010)

optimal for a species, termites do not modify their construction strategy and type.

The termite mounds – First, it was important that the termite mounds were both far from carbonate outcrops, in order to limit the influence of pH and calcium ion on aggregation of clays and organic matter (Rowley et al., 2018). Finally, the field area was also chosen because of its absence of sodic sediments.

The epigeal termite mound built on sand-size parent material has a diameter of 4 m and a height aboveground of 2 m. It was probably built between 4 and 8 years ago, was abandoned a couple of times, but has always been recolonized by the same termite species. The epigeal termite mound built on fine silt-size material has a diameter of 1.5 m and is 1 m high aboveground. The mound is more than two years old, was continuously used by termites, and was still occupied during this study. The same species (i.e. *Macrotermes michaelseni*) as in the sandy area is living in this mound.

2.2. Sampling strategy

As it is the case in numerous studies on fungus-growing termites, a trade-off has to be made between the number of mounds to be studied and the number of samples to be collected per mounds (Erens et al., 2015). A restricted number of samples collected in each mound would have limited the generalization of the conclusions. Conversely, a large number of samples collected in each mound would allow detailed variations to be assessed. Therefore, both mounds were sampled at high resolution, with 84 and 64 samples collected, added with their adjacent control soil.

Sampling took place during two field campaigns, in September 2017 and 2018 (during the dry season). The aboveground parts of both termite mounds were excavated in 2017 in the following manner. First, a systematic sampling was carried out on the two adjacent control sediments at depths of 5 cm, 10 cm, 20 cm, 40 cm, and 80 cm belowground. For the termite mound on sand, a 60 cm wide trench was dug along an east-west axis through the centre of the mound. The sampling started 6 m away from the mound centre and a sample from the surface of the mound was collected at a regular distance of 1 m in the direction of the mound centre. At each 1 m-interval, samples were also collected at each 25 cm-interval in depth until reaching the ground level. For the termite mound developed on silts, the sampling started 1 m from the centre and then each 20 cm until reaching the centre of the termite mound. Each point was systematically sampled at the surface and at each 20 cm-interval in depth until reaching the ground level. The belowground parts of both mounds were sampled during the 2018 campaign. The termite mound on sands was flattened to the ground level reached the preceding year. Then, sampling was systematically performed outward from the centre of the mound along the four compass points at 50 cm intervals. At each of these points, a 2-m long auger was used in order to reach the basal parts of the mound 2 m below the ground, allowing the various depths to be sampled. For the termite mound on silts, the procedure was the same: the mound was flattened and then systematically sampled from the centre towards the exterior every 20 cm in the four cardinal directions. The process was repeated in the same manner using an auger in order to reach a depth of 1 m below the ground, allowing the various depths to be sampled.

This sampling strategy aimed at collecting samples for the particle-size distribution analyses, which reflect the diversity of the various parts of the two respective mounds. In addition, Kubiena boxes were used to sample termite mounds and control sediments for thin section descriptions. In total, 148 samples were collected from both mounds and 20 from the control sediments for laboratory analyses. Moreover, 18 thin sections from the mounds and 6 from the control sediments have been made at the *Servizi per la Geologia*, Piombino, Italy (Dr M. Sbrana). Consequently, thin sections were used to cross-check conclusions drawn from blind and destructive laboratory analyses regarding patterns (Francis et al., 2012).

2.3. Laboratory methods

Grain-size distribution – Grain-size analyses were performed on soil and sediment samples after treatment with 10% hydrochloric acid (HCL) in order to remove the carbonate fraction. The residual material was washed and treated with 35% hydrogen peroxide (H_2O_2) in a water bath at 45 °C to remove organic matter. Clay destruction was avoided by a regular pH control (pH 7–8). The reaction was stopped after one week and the excessive hydrogen peroxide was evaporated. A dispersal agent (Na-hexametaphosphate; 40 g/L) was added to the samples, which were then shaken during 12 h before analysing. Grain-size measurements were performed using laser diffraction (Beckmann Coulter LS 13 320) and the Fraunhofer approximation was applied. Grain-size percentages are expressed by the relative volume percentage defined by Pansu et al. (2003).

Thin sections observations – Thin section observations were used to identify biogenic impacts on the termite mound formation and to highlight the differences between their sediments and the ones observed in the landscape. Particular attention was paid to quartz size, shape, and abundance, as well as to their distribution pattern within the ground-mass, as these aspects reflect modifications brought by termite activities. Closer observations were conducted in order to identify features induced by fungus-growing termites' bioturbation. Thin section observations were also used to support the conclusions drawn from the grain-size analyses performed on the coarse and fine sediments of the parent material and to identify the adjustments brought by termites to these materials within their respective termitarium. The thin sections were observed using an Olympus BX53 polarized light microscope, which allows for plane polarized light (PPL) or cross polarized light (XPL) observations at various magnifications. Microphotographs were taken on the same microscope using an Olympus DP26 camera and captured through the program CellSens Standard. The vocabulary used in the description of the thin sections was adapted from Stoops (2003). Stoops et al. (2018) was the main reference for the identification and interpretation of micromorphological features.

X-ray diffraction – The mineralogical composition was determined using X-ray diffraction (XRD) on the bulk, coarse silt (16–50 μm), fine silt (2–16 μm), and clay (<2 μm) fractions of soil and sediment samples (Adatte et al., 1996), using an ARL Xtra diffractometer (Thermo). The bulk composition was measured on the sample powder compressed in holders. The peak intensities of major minerals were converted into relative abundances, according to external standards. Amorphous or poorly crystallized minerals (i.e., various iron oxides and some phyllosilicates) are included in the non-quantified fraction. Regarding the fine silt and clay fractions, 2 mm-sieved soil and sediment samples were treated with 10% HCL in an ultra-sonic bath for 3 min in order to remove carbonate. Both fractions were separated by centrifugation and deposited on distinct glass plates. Samples were glycolated before XRD analysis to detect swelling clay minerals.

Processing of *grain-size data* – The processing workflow of data pursued two different goals. First, data were processed in order to confirm the differences between the various position groups of samples from the two mounds (above- and belowground, control soils) by using the various modes of their grain-size distributions (all curves are multimodal). The objective was to identify the various groups of curve shapes and, therefore, to clearly value the effect of the sediment location. Based on these results, the second aim was to identify the origin of the sediments constituting the different parts of the mounds. This second objective also included the comparison of the mounds with control soils in order to assess the contribution of termites in the change of grain-size distributions.

First, all the grain-size distribution curves were plotted on the same graph in order to observe the overall variations of their shapes. Then, as the 140 curves were all multimodal, but displaying similar modes with various amplitudes, they were processed using a mode detection algorithm with Matlab™ R2017b in order to group them. As expected, the

distribution of modes expressed a clustering of the curves according to their three different origins (control soils, coarse and fine mounds) and respective positions in the mounds (aboveground or belowground; see Fig. 2A–D). After the confirmation of the pertinence of the topographic nomenclature by the distribution of the mode amplitudes, a median curve was calculated for each curve set (Fig. 2). These median curves were then processed with Matlab™ R2017b in order to identify their respective modes with precision, to check if these were or not repetitive, and therefore significant in terms of sedimentary signal. Five main and

repetitive modes were recognized. They constituted a first clue in the identification of the origins of sources forming the unconsolidated sediments of the Chobe Enclave District.

The next step involved an End-Member Mixing Analysis (EMMA). EMMA was performed based on the algorithm provided by Dietze et al. (2012) and run with Matlab™ R2017b (9.3.0.713579). It was applied to all the grain-size distribution curves (coarse and fine grain mounds as well as control soils) in order to identify the possible sources of sediments that could have contributed to the various soil and mound

Fig. 2:. Flow chart of the methods used to assess the diversity of the grain-size distributions. (A) Grain-size distribution curves of all samples from the fine grain mound (as an example). (B–D) Different groups have been identified based on the curve similarity (supported by mode detection in Matlab®). For each group, the median curve is computed. (E) Common modes are selected using the five median curves corresponding to five groups. (F) Grain-size distributions are processed in an End-Member Mixing Analysis (EMMA) using Matlab® software. This analysis results in the identification of five main End-Members (EM1 to 5). (G) Bar chart showing each sample with the associated contribution of each End-Member (EM1 to 5 in %).
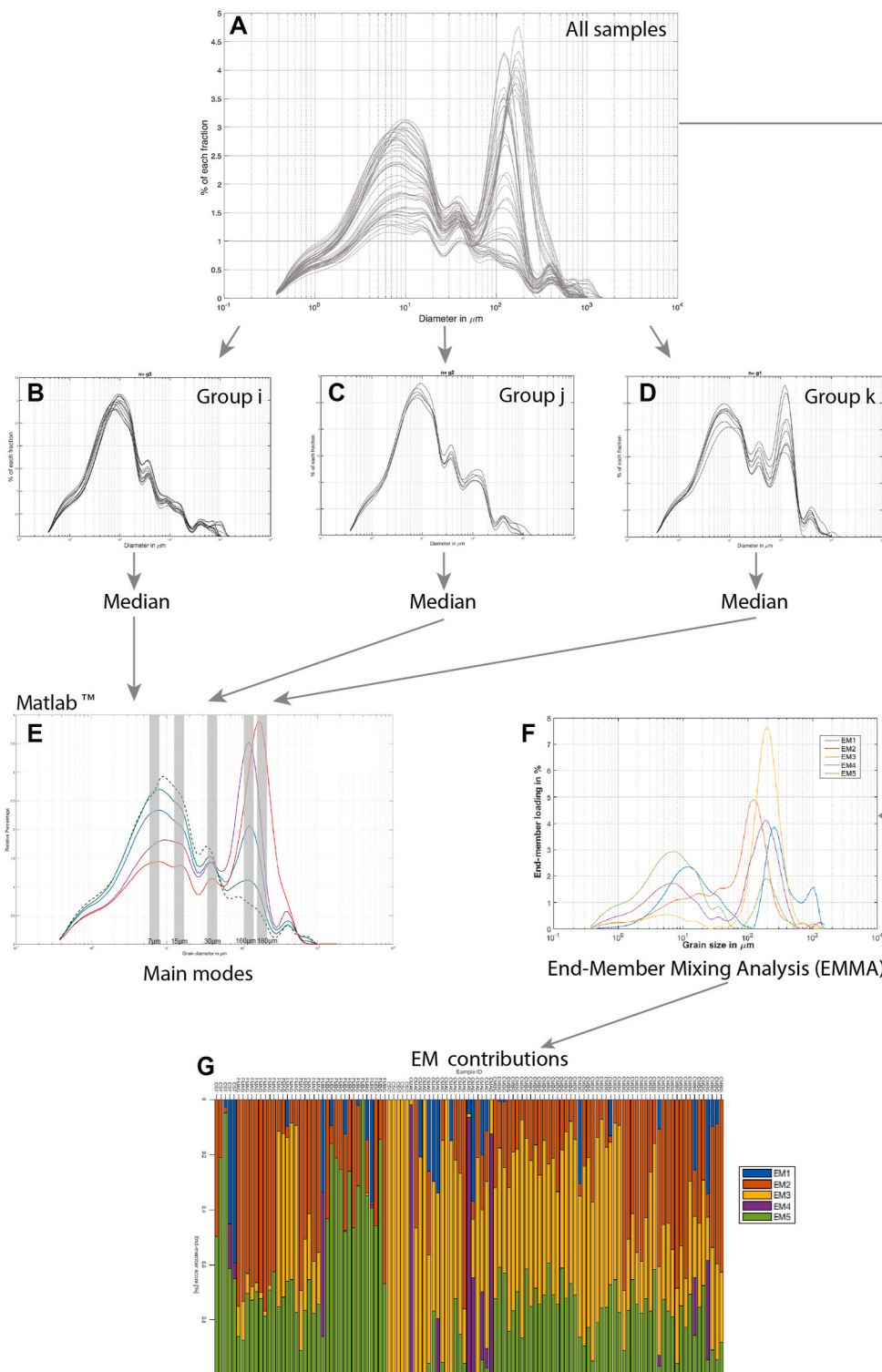
samples. Based on the eigenvector values, it was decided to keep five end-members, which explained 97% of the total variance. Adding a group would have changed the explained variance by only 1% but would also have added more confusion.

3. Results

3.1. Grain-size distributions and sediment sources

Identification of the main sedimentary contributions – Based on the detection and variability of mode amplitudes, it was possible to separate two groups inside each of the above- and belowground sets of curves, in
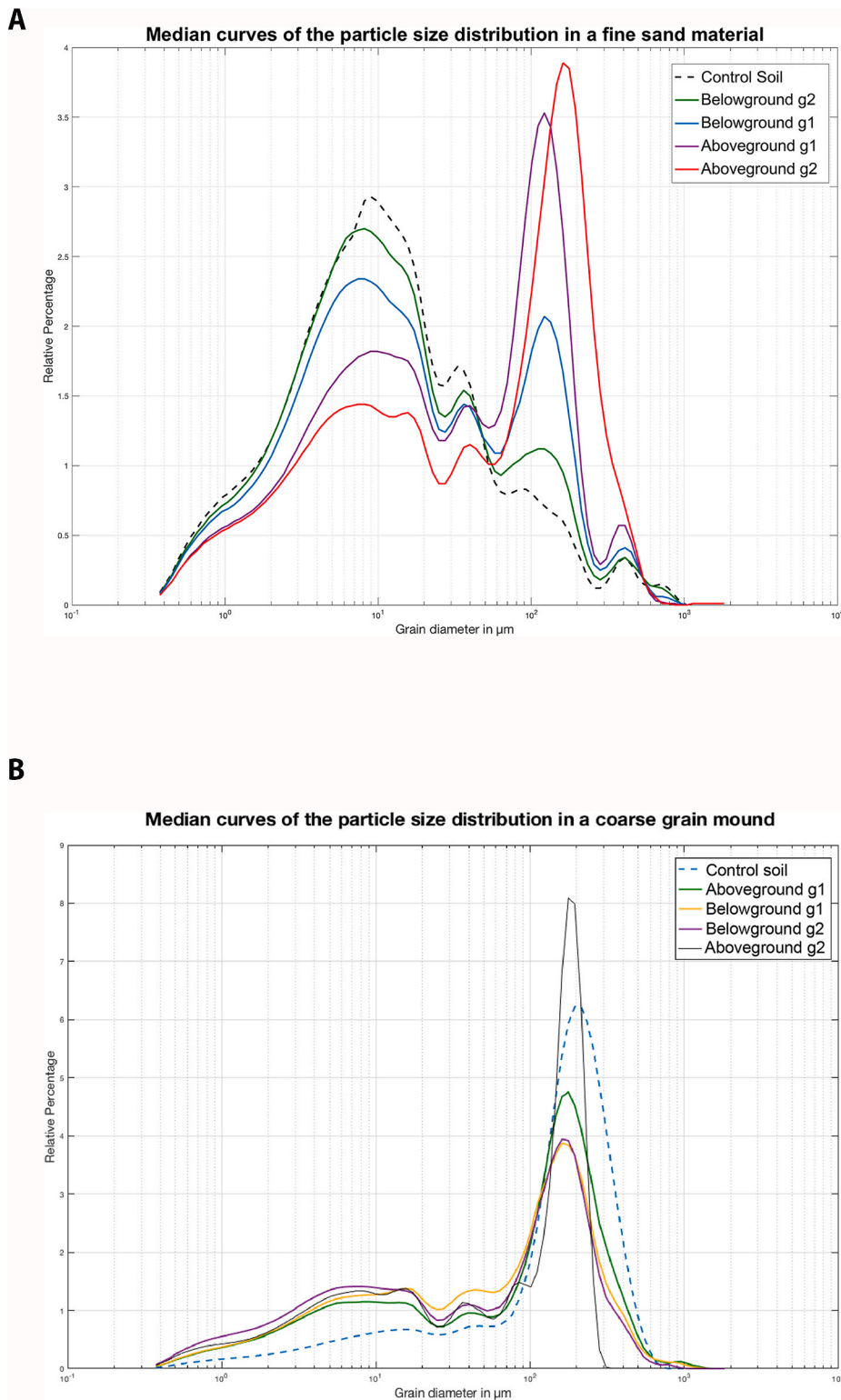

Fig. 3:. Median curves of the grain-size distributions measured in each group of samples: (A) Data from termitarium built on silt-size parent material; (B) Data from termitarium built on sand-size parent material (*Aboveground g2* = Infilled cavity made by another animal than termites).

addition to the control soils. Once the ten homogenized curve groups were identified (one control soil, two aboveground and two belowground groups for the fine and coarse grain mounds), the median curve was calculated for each of them (Figs. 2 and 3A, B). Using the same mode detection algorithm, five preeminent modes were recognized in each of the ten median curves, which are: a sand mode (180 µm or Φ 2.5), a fine sand mode (160 µm or Φ 3.1), a coarse silt mode (30 µm or Φ 4.8), a silt mode (15 µm or Φ 6.1), and finally a fine silt one (7 µm or Φ 7.1).

EMMA results (Fig. 4A) clearly show five sedimentary contributors (from EM1 to EM5) to the total variance of the mound grain sizes. In EM1, two distinct groups appear: one with a mode in the silt fraction at 15 µm and one in the sandy fraction at 250 µm. Both groups are clearly separated at 120 µm. The EM2 curve displays a net skewness with most of its distribution concentrated on the right side with a mode at 120 µm. A minor mode is present at 35 µm. The EM3 curve has a leptokurtic shape with a mode at 200 µm and a minor platykurtic distribution centred at 7 µm. In the EM4 curve, two populations stand out, one at 7 µm with a mesokurtic shape and the other at 200 µm with a leptokurtic shape; the populations are not well separated, a bulge is also observable at 35 µm. The EM5 curve shows two distinguishable populations, one at 7 µm and the other at 200 µm; they are separated at 70 µm. As for the three other curves, a bump is displayed at 35 µm.

Grain-size distribution in the termite mound on silty material – The presence of five distinctive groups of particle size distributions (Fig. 3A) is confirmed by the EMMA, except for the *Belowground fine g1* and *g2*, which are partly mingled (Fig. 4B). First, the control soil is characterized by a large predominance of the fine to very fine fractions, as expected (Fig. 3A). This soil is mainly characterized by EM5 and EM2 in its top part, whereas in its bottom part, it is EM5 and EM1. Second, a transition

is observed from the initial parent soil towards the belowground parts of the mound, which are enriched in sandy material. It is necessary to stipulate that some of the belowground samples are related to galleries and fungus-chambers, this material being slightly coarser (identified as *Belowground g2*, which is characterized by the presence of EM 1 and EM5). This contribution of the coarse fraction increases in the *Belowground g1* formed by termitarium samples, including a new contribution from EM 2 (Fig. 4B). The coarse fraction towards sand increases in the central upper part of the mound (*Aboveground g1* identified by the predominance of EM2) to finally reach a maximum in the apron of the mound (*Aboveground g2* characterized by the higher proportion of EM3; Fig. 4B).

Grain-size distribution in the termite mound on sandy material – The presence of distinctive groups of particle-size distributions (Fig. 3B) is confirmed by the EMMA as well. First, the control soil is characterized by mainly the sandy fractions, as expected (Fig. 3B). This soil is solely under the influence of the EM3 (Fig. 4B). Second, a new transition is observed from the initial parent soil to the mound, which is enriched in fine material <20 µm. Overall, the aboveground samples are mainly characterized by the absence of EM5, which describes fine material. The *Aboveground g2* is associated to an infilled gallery and its specific characteristics will be examined in the Discussion section. In the belowground samples, the EM2 fraction increases substantially from group 2 to group 1 (Fig. 4B).

After this characterization of the various groups forming the termitaria, a question is still pending: are there common grain-size sources in the two termite mounds? EMMA results (Fig. 4B) clearly show an evolution of the grain-size distributions inside each mound, from the control soil (supposed to be the parent material that existed before the termite
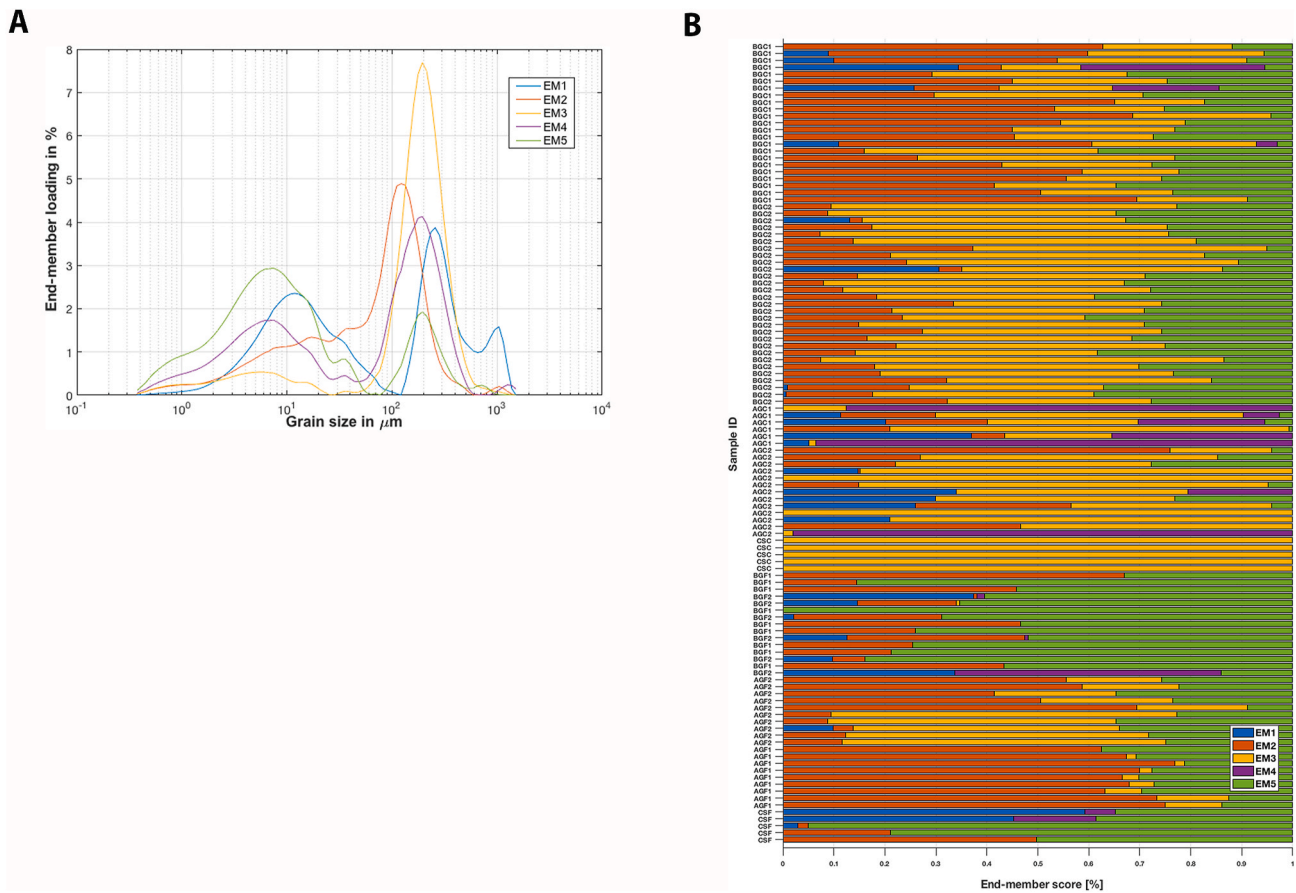

Fig. 4. (A) Particle-Size Dsitribution (PSD) plot of end-members; (B) Bar chart of the end-member contributions to each sample. Control soil fine = CSF; Aboveground fine group 1 = AGF1; Aboveground fine group 2 = AGF2; Belowground fine group 1 = BGF1; Belowground fine group 2 = BGF2; Control soil coarse = CSC; Aboveground coarse group 1 = AGC1; Aboveground group 2 = AGC2; Belowground coarse group 1 = BGC1; Belowground coarse group 2 = BGC2.

settlement), to the various compartments of the termitaria. But EMMA (Fig. 4B) also emphasizes that the selected modes and end-members can be successfully used to characterize the variability of the curves (Figs. 3 and 4), whatever their origin. Consequently, this result raises the question of possible common sources of some of the mixed sedimentary sources, but these latter would be used in different proportions by the termites during the mound building and its evolution through time, an hypothesis illustrated and discussed below.

3.2. The diversity of minerals in the mounds

The comparison of grain-size distributions between the two termitaria built on distinct substrata clearly demonstrated differences in terms of textures, but also included some common sources. But what are the differences in their mineralogy? Do termites change the mineral composition of their mounds compared to their control soils? Does the mineralogy vary with the grain-size distributions, i.e. between mounds? To answer these questions, XRD analyses were performed on the bulk

mineral fraction of the above- and belowground parts of the fine and coarse grain mounds, as well as on their respective control soils. Results showed that most of the samples originating from the different sampling groups of the mounds display a clear mineralogical homogeneity. Only control soils include significant differences in mineral proportions. Consequently, six examples are provided in Fig. 5A to illustrate the mineralogical diversity of mounds, in addition to the control soils. XRD analyses were performed on the bulk fraction of samples also used for thin section observations in order to compare the main minerals detected by XRD with the minerals present in thin sections. Most of the detected peaks clearly correspond to quartz, which is present in all samples but in different proportions. Calcite is the only mineral that is absent from both control soils, but present in the above and below parts of the coarse grain mound (Fig. S1A). Watson (1969) imputed the elevated concentration of calcium to a process termed "differential leaching", outlining that termite mounds are generally less leached than their respective control soils. Complementary arguments were put forward by Watson (1975) suggesting that the increase in Ca contents in
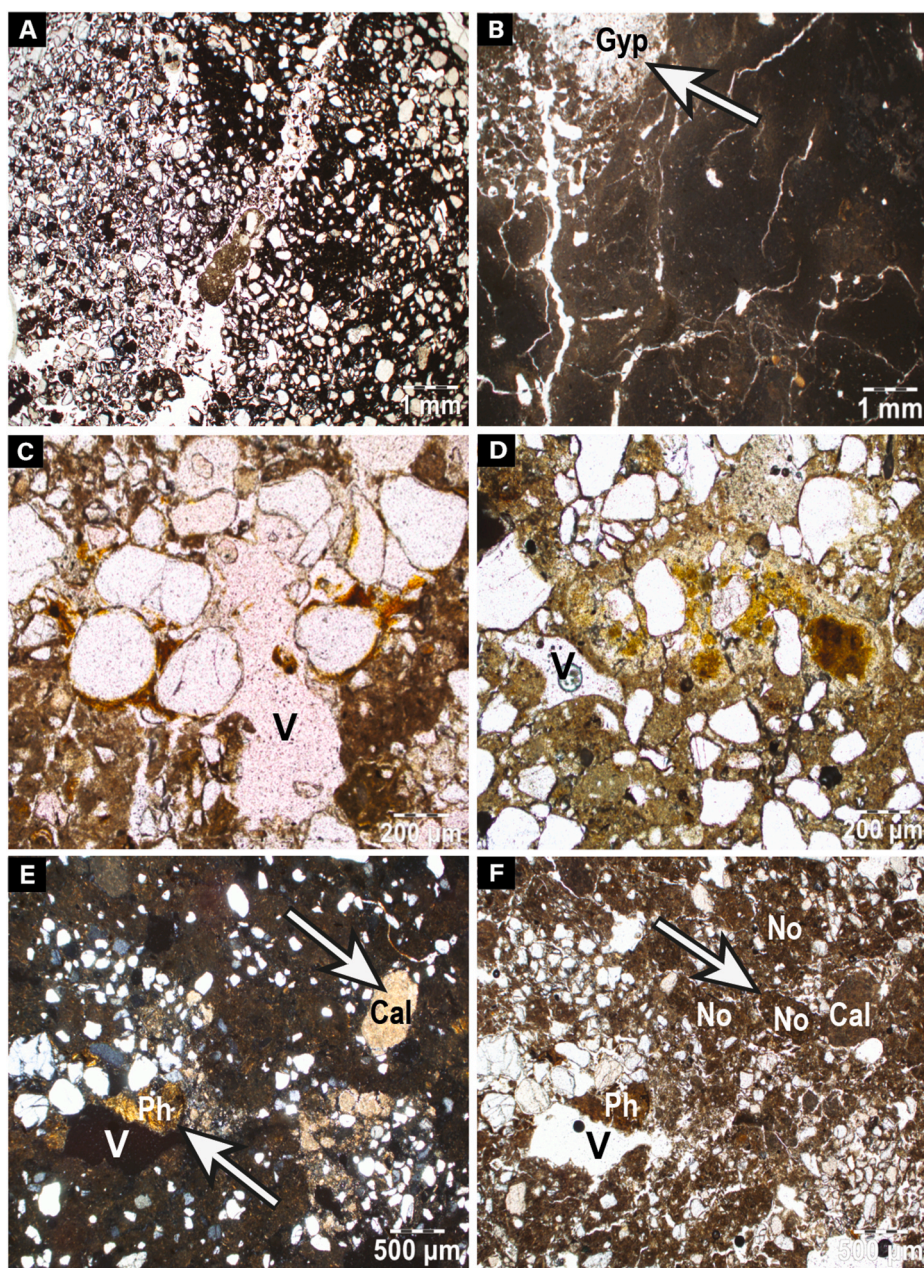

Fig. 5. (A) Control soil of the coarse grain mound in plane polarized light (PPL), with a single-to double-spaced fine to equal enaulic c/f distribution. In this case, the micromass is not the dominant fraction. The coarse fraction comprises sub-rounded and sub-angular quartz grains typical of the region. (B) General appearance of the fine grain mound control soil in PPL. Dark compact micromass containing some clays, interrupted by channels, chambers and planar voids. A large gypsum crystal is visible at the top left inside the chamber (Gyp and arrow). (C) Gefuric and porphyric c/f distributions in the fine grain mound (view in PPL). In the middle, coarse rounded and sub-rounded quartz grains are coated and bridged by orange clays (gefuric c/f distribution). At the top and bottom of the microphotograph, small sub-angular quartz grains are included in a brown micromass (porphyric c/f distribution). V: void. (D) PPL view of the aboveground part of the coarse grain mound. Single spaced porphyric c/f distribution with large sub-angular quartz grains, micrite, and possible phosphate grains. (E) Cross polarized light (XPL) view. Extinct micromass embedding sub-rounded quartz, calcite (Cal and arrow) and possibly phosphate grains (Ph with arrow) inside the fine grain mound. The micromass displays a faint circular-striated b-fabric. (F) Same view in PPL. The micromass is characterized by a porphyric c/f distribution with a low sorted coarse quartz fraction. Some allothic nodules (No and arrow) can be observed. (For interpretation of the references to color in this figure legend, the reader is referred to the Web version of this article.)

Macrotermes mounds might stem from consumed plant tissues. The origin of carbonate accumulation in fungus-growing termite mounds can be seen as a result of complex pedogenic processes involving both indirect biotic action of bacteria, fungi, and plants (i.e. as sources of carbon and alkalinity) and abiotic reactions (e.g. leaching processes, dissolution-precipitation of crystals) with the highest concentration around the hive centre. Erens et al. (2015) attributed the presence of higher proportions of carbonate in the lower part of the mounds to the dissolution in their upper parts and leaching downward, where CaCO$_3$ reprecipitates. Their distribution pattern appeared to be similar to those of the pH. Moreover, the mineralogy of the mounds remains similar in terms of accessory minerals (feldspars, iron oxyhydroxides, calcite, and an amorphous material, probably amorphous silica; see next section on soil micromorphology of mounds).

Results from the end-member mixing analysis (Fig. 4) showed a minor 35 μm mode between the two main sources. This mode was naturally also observed in the median curves of the grain-size distributions (Fig. 3), this fraction being encountered in both mounds. Thus, XRD analyses were performed on the 16–50 μm fraction of the fine grain mound (Fig. S1B) in order to confirm the nature of the minerals composing this fraction. Two peaks in the XRD diffractogram (Fig. S1B) are identified as sepiolite. Kaolinite is detected in the control soil and the aboveground part of the fine grain mound, as well as in the belowground part of the mound. Quartz is found in the above- and belowground parts of the fine grain mound and the control soil. Traces of mica are also present in all samples as well.

3.3. A micromorphological approach to mound fabrics

Coarse fraction of the groundmass – Quartz grains are always present in the groundmass, ranging in size from tens of μm to around 500 μm (Fig. 5A). Other minerals are generally small, heavily weathered, or present only in trace quantities, with one notable exception, gypsum. Gypsum crystals were found in the fine grain mound and its control soil (Fig. 5B). The control soil near the fine grain mound shows the least presence of quartz, representing generally <30% of the components and 5% or less in the uppermost samples. Quartz grains are sub-angular in shape, generally <100 μm long, and rarely >250 μm. The control soil of the coarse grain mound has an intermediate composition, with quartz representing 50–70% of the groundmass. In these samples, the greatest grain-size variation is observed, from around 10 μm up to 500 μm; grains are poorly sorted. The shape of the grains seems to correlate with their size, the smaller ones are often angular while the bigger ones are often sub-rounded or well rounded. (Fig. 5A, C). In soils inside both mounds, the groundmass is always comprised of at least 40–50% of quartz grains, the sizes of the grains tending to vary within each sample from tens of micrometers to 500 μm with no clear trend between samples or mounds. The shape is also variable as, in the same sample, rounded and angular grains may be found; but, the most abundant shape across all samples remains the sub-angular type.

Micromass – In the control soil of the fine grain mound, the micromass is the dominant fraction (70–90%) of the groundmass. It is a homogeneous and compact brown mass in PPL, with slightly orange-yellowish patches (Fig. 5B). In XPL, its b-fabric has low limpidity with cloudy patches and is striated, in particular in areas coinciding with the orange-yellowish patches seen in PPL. The striated areas appear yellow and display a moving extinction. Inside the fine grain mound, the micromass is similar to that of its control soil; it has the same brown color and a circular-striated b-fabric. Its color under PPL can vary between dark brown (almost black) and a lighter orange-brown. In XPL, the b-fabric can be either completely opaque and extinct, or almost beige and light orange. In the control soil of the coarse grain mound, the micromass is not the dominant fraction (only 30–40%). In PPL, it has a very dark brown color, and in XPL, it is homogeneously opaque and extinct. In the coarse grain mound, the micromass has an almost greenish- or yellowish-brown color in PPL (Fig. 5D), while in XPL, it is

mostly opaque with a slightly crystallitic or speckled b-fabric.

The fine grain mound and its control soil contain visible clays (Fig. 5E) and sometimes, iron oxyhydroxides. Some clays are also visible in the micromass of the coarse grain mound. Contrary to clays, calcite is relegated to mound samples and is not found in the respective control soils. In addition, mounds present a different ratio of quartz grains to micromass when compared to their control soils. For example, the coarse grain mound's control soil displays a low proportion of micromass (Fig. 5A), while inside the mound, the micromass constitutes an important portion of the groundmass (Fig. 5D).

Fabric – The fine grain mound's control soil displays a double-spaced porphyric c/f distribution and widely spaced plane voids, modified plane voids, channels, and millimetric chambers. Inside the fine grain mound, aggregates with different c/f distributions can be observed, from double-spaced open porphyric to closed porphyric, but also gefuric (Fig. 5C); these aggregates are usually elongated and millimetric and are arranged in a banded pattern. Vughs between aggregates are common, as are channels and chambers (Fig. 5C). The coarse grain mound's control soil has an enaulic c/f distribution and with small packing voids between quartz grains (~10 μm) and larger vughs (hundreds of micrometers) between aggregates of micromass and grains. In the coarse grain mound, grains and micromass are generally randomly distributed and well aggregated, constituting a single-space porphyric c/f distribution (Fig. 5D). In some areas, the c/f distribution may tend more towards the enaulic type with complex packing voids. Chambers and channels are often visible.

Structure in the fine grain mound – One of the most striking features observed in the samples is certainly the banded arrangement of the microstructure found inside the fine grain mound (Fig. S2A). This arrangement may be what Mermut et al. (1984) described as "lamellar fabric" in sandy and silty termite mounds.

To summarize, important textural differences are observed between the control soils and the mounds. This is particularly conspicuous in the transition from silt to sand, in the fine sand mound (Figs. 3, 4B, and S2), and from sand to silt, in the coarse sand mound. In terms of mineralogy, the main contrasts between samples are between the proportions of phyllosilicates and quartz, as well as the presence of calcite in the coarse sand mound compared to its control soil. Both of these differences are also seen in the thin sections (e.g. Fig. 5 and Fig. S2). Another difference observed in thin sections is the similar ratio of coarse to fine material throughout the mounds, a property not observed in the control soils. Nevertheless, some questions remain unresolved: is there a possible common source of the mixed sedimentary sources? Are there common grain-size sources in the two mounds? Are these sources used in different proportions by termites during mound building? In other words, it is hypothesized that termites can change the textural compositions of their mounds, compared to their control soils, to obtain an optimum grain-size distribution for the colony.

4. Discussion

First, it can be assumed that, for each of the sedimentary source identified during data processing, there is a corresponding specific source found in the subtropical landscape of the Chobe Enclave District. Each source can be attributed either to regionals sands, i.e. kalahari sand (allochthonous) or to the parent material, e.g. diatomites (autochthonous). These main sedimentary sources from different sources can be mixed in various proportions to provide the observed grain-size distributions. Indeed, results show that both mounds contain the same groups of grain-size contributors. But their respective proportions in the mounds, as well as in their distinct parts, vary for different reasons, which are discussed in the following section.

4.1. The nature of the sources and their respective origin

Kalahari sands –These sands form the prominent sedimentary source,

characterized by the modes displayed at various values between 125 and 200 μm (Fig. 3A and B), and are perfectly represented by the end-member EM3 (Fig. 4A). The presence of such a diversity in the KS is explained by the variety of the reworking intensities related to their settings, e.g. dunes, floodplains, slopes undergoing runoff, etc., as supported by the end-members (Fig. 4A) and the thin sections (Fig. 5). Nevertheless, although KS underwent many erosions and reworkings, they still preserve their leptokurtic grain-size distributions with specific modes, testifying their complex history.

Dust and desert loess – The sediments from the mounds include a loess fraction. Indeed, one of the components of the grain-size distributions fills all the requested criteria: (i) the Chobe Enclave District is far from glaciated regions; (ii) the identified sources are not more than 300 km as stipulated above; (iii) sources and loess have similar mineralogical compositions (quartz, amorphous silica, and kaolinite; Fig. S1A and B); (iv) and the source is located upwind as expected; (v) in addition to the four criteria from Crouvi et al. (2010), the grain-size distribution spans from 30 to 50 μm as expected (Fig. 3A, B and S2). These populations obviously contribute to the various end-members, with the highest influence on EM4 and EM5 (Fig. 4A). In conclusion, the two mounds not only share a KS component, but also integrate a loess and dust fraction.

Diatomite mud – Observed with a scanning electron microscope (see Fig. S3), the diatomaceous earths include only a few intact diatoms compared to the number of fragments, crushed and broken frustules. Consequently, their grain-size distributions display two subsets: one with a mode between 10 μm and 20 μm, corresponding to a population of fairly complete and preserved frustules, and another, usually <7 μm, associated to a platykurtic curve, reflecting the mix of broken and crushed fragments of diatoms. The two subsets can be observed in both mounds (Fig. 3A and B), as well as in the end-members. Indeed, EM1 accurately represents the contribution of a potential intact population of frustules, whereas EM5 displays the platykurtic curve of a diatomaceous mud of poorly sorted fragments (Fig. 4A). Moreover, all the grain-size distribution curves feature a shoulder between approximatively 1 and 2 μm (Fig. 3A and B and 4A). Two hypotheses can explain this grain-size interval: (i) very fine diatom fragments as mentioned above, or (ii) clay minerals, one not excluding the other. Indeed, in tropical regions, Michalopoulos et al. (2000) observed that diatom frustules can be converted into various forms of clays during the burial and early diagenesis, the dominant newformed minerals having a composition similar to K-smectite. These transformations of biogenic silica into authigenic clays were observed in marine deltaic deposits, but the continental deltaic sediments of the Chobe Enclave did not necessarily provide significant different conditions. The fine grain mound developed on diatomite, as well as its control soil, include sepiolite in the fine silt fraction (Fig. S1B and Fig. S2). This mineral, which is authigenic in the Chobe Enclave (Fig. S3B), likely contributes to the <2 μm fraction detected by grain-size analysis.

Distal fluvial silts – Another source for the fine silt fraction can be attributed to allochthonous sediments from the Angolan highlands. Sediments deposited south of the study area have an average grain size of only 10 μm (Gamrod, 2009). In the context of the vast Okavango Delta's swamps, the water velocity decreases the sand-size of the transported fraction: it was estimated that up to 90% of the sand-size material is deposited when entering the panhandle region of the Delta (McCarthy and Metcalfe, 1990). This process enables coarse sands to be stored upstream and silts to be deposited downstream. Consequently, distality from the upstream part of the panhandle is an important component in the grain-size distribution equation. For example, in the control soil of the coarse grain mound, no diatomite was found, but a fine silt fraction is present. In this case, the source of this fine non-diatomaceous earth silt could be attributed to a distal entry point situated between the Linyanti Swamp (along the Kwando river) and the Angolan highlands.

In conclusion, as emphasized in this section, each part of the mound is composed of a mixture of one or more grain size, with each corresponding to a specific source. Therefore, one or more sources have contributed to each specific area of a mound. The different grain-size populations identified in the end-members (Fig. 4A) and the particle-size distributions (Fig. 3A and B) can therefore be interpreted as follows: the >2 μm and <7 μm modes can originate from distal fine silts or broken frustules, the modes centred at 15 μm refer to diatomaceous earth and the 35 μm mode to dust and desert loess. Finally, the 120 μm, 200 μm and 250 μm modes illustrate the diversity of dynamics undergone by the Kalahari Sands. Consequently, the fine grain mound should have been developed from mainly distal fine silts, clays, and diatomaceous earth in addition to some desert loess and Kalahari Sands. The proportions between these sources vary depending on the part of the mound considered. Therefore, the coarse grain mound includes the same grain-size populations as in the fine grain mound, but with varying proportions for each contribution, depending on the location inside the mound and, of course, the effect of termites.

4.2. End -member mixing analysis of the mounds and their parts

EMMA's data show that two modal grain-size populations are roughly represented in the five groups, dominated by a silt or a sand fraction illustrated by the two extremes, EM5 and EM3 curves, respectively (Fig. 4A). The analysis of the end-member scores (given in percentage; Fig. 4B), emphasizes that each control soil corresponds to a specific group. Based on the preceding section, the control soil of the coarse grain mound appears almost exclusively composed by sands, its unique contributor, the EM 3, being explained by the presence of well-sorted Kalahari Sands. Regarding the control soil of the fine grain mound, its composition is more complex. Although EM5 remains the main contributor, some samples are also influenced by EM1, or in a minor extent, by EM2. All these end-members include a sand fraction, which is not surprising due to the omnipresence of KS. But EM1 and EM5 contain dominant fine fractions, which refer to the diatomaceous earth, as expected. On the other hand, the contribution of EM2 emphasizes a sand input in the top horizons, although the diatomaceous fraction dominates.

Regarding the mounds, the proportion of each end-member contribution depends on building requirements of fungus-growing termites, and can be qualified as the imprint of termites. The percentage of EM contributions in each specific areas of the mounds, Aboveground Fine group 1 and group 2, Belowground Fine group 1 and group 2, Aboveground Coarse group 1 and group 2, Belowground Coarse group 1 and group 2 (AGF1, AGF2; BGF1, BGF2; AGC1, AGC2; BGC1, BGC2), varies with the material required for the different parts of the mounds, whatever the granulometric context.

The shoulders and peaks observed above 400 μm in end-members (e. g. at 1000 μm in EM1) cannot be attributed to the KS: after checking the absence of potential technical artefact, it seems reasonable to interpret it as the presence of some coarse grains of amorphous silica (Ringrose et al., 2008). The mode detected at 35 μm in the five end-members has already clearly been attributed to desert loess. Therefore, it is not surprising to find it as a common component of end-members.

4.3. Variability in sources: from parent material to termite input

Grain-size distributions in the termite mound on sandy material – As demonstrated above, the Kalahari Sands constitute the parent material of the coarse grain mound. In the aboveground part of the coarse grain mound, termites tend to add a minor amount of fine material as shown by the contributions of the various end-members (Fig. 4B), although a contribution from airborne dust cannot be discounted. In addition, a cavity was identified in the upper part of the mound. This cavity, or gallery of unknown origin, likely made by a predator, has been infilled by very well sorted Kalahari Sands (end-member EM3 up to 85%), dust and desert loess (with the weight of end-members EM1, EM2, and EM5 up to 35%, 76%, and 28%, respectively). This material was later mixed

by bioturbation, erosion, and/or gravity with the original building mound material to produce this unique *Aboveground g2* curve (Fig. 3B). In the belowground part, termites added a significant quantity of fine material (Fig. 4B). Termites got this fine material either from the small fraction of fine silt and clay contained in the sands of the control soil (such fractions were detected in it; Fig. 3B) or from deep sediments under the mound. Indeed, originally, the control soil of the coarse grain mound is extremely homogenous, with the dominant presence of KS (end-member EM3) and only minor amounts of fine silts, attributed to a distal source (see above; Fig. 4A and B). In conclusion, the grain-size distributions inside the mound differ radically from the control soil with an increasing impact of EM2 and EM5.

Grain-size distributions in the termite mound on silty material – The control soil developed on diatomite muds is significantly influenced by end-members EM5, EM1, and EM2. Surprisingly, the end-member EM3 is totally absent. In the belowground part, termites tend to add fine sand (end-member EM2), but not the coarser end-member EM3. Termites get this fine sand either from the fine sand fraction contained in the control soil, or from deep sediments from under the mound. Regarding the aboveground part of the termitarium, it is necessary to distinguish between the *Aboveground g1* and *g2*. Indeed, termites tend to add a fine sand to the *Aboveground g1*, which corresponds to the centre of the termitarium (central column of the mound): the EM2 group contributes to up to 75% to *Aboveground g1*. Concerning the other aboveground part, i.e. the apron (*Aboveground g2*), termites probably added some quantity of end-member EM3 (up to 63%). But it is reasonable to think that another possible and significant contribution can be related to sand saltation around the mound. In conclusion, this mound shows a massive shift from a total absence of end-member EM3 to up to two-thirds of the total contributions (Fig. 4B). If all aboveground samples are considered, the share of the sand fraction inputs of EM2 and EM3 combined are >65%.

In both termitaria the transport distance of the selected material by termites remains in the vicinity of the mounds i.e. 50 m. *Macrotermes michaelseni* species tend to forage for food purposes at a maximum of 50–100 m distance from the mound. For sand grains collection the horizontal distances travelled by termites can reach similar values especially for the coarser sediments, but for the clay fraction the tendencies for termites will be to dig in the ground, in most cases not more than a meter deep (Jouquet et al., 2017), but in certain circumstances e. g. to reach the water table, termites might go down 10–20 m deep or more (West 1970). The way termites build their mound is based on a templating odor at the nest level that undergoes diffusion and advection globally throughout the mound. Each termite carrying sand grains back to the mound will deliver them in a deposit center pre-assigned by the deposition of a building pheromone at the local level. These depot centers are always very close to where the building takes place in the various compartments of the mound (Ocko et al., 2019).

4.4. Towards optimizing grain-size distributions in fungus-growing termites' termiteria

The fine fraction (clays and silts) forming the micromass of the thin sections (Fig. 5C) were also revealed in the grain-size distribution median curves for both mounds. Similarly, variations in the quartz grain distributions were clearly observed in thin sections. By comparing thin sections and grain-size distributions, it appears that termites can add variable amounts of quartz particles in order to build the different parts of their mounds. (Fig. S2). Regarding the banded arrangement of the microstructure found in the fine grain mound and described above, (i) it is not observed in the corresponding control soil, but (ii) only in thin sections sampled in an active termite mound, and (iii) it is always associated with markers of termite presence (i.e. termite excrements). Therefore, it is proposed that termites are the agents responsible in the development of such a specific "lamellar fabric" of the microstructure (Fig. S2A).

Termite activity obviously affected grain-size distributions, mineralogical compositions, and basic fabric dispersal in the soil (see Fig. S2). Indeed, fungus-growing termites reach a coarser fraction/texture in the aboveground, and a finer fraction/texture in the belowground parts of their respective mound. Once abandoned and destroyed by erosion, the mounds modify the grain-size distribution of the sediment on which they developed, changing the sedimentological parameters of the geological formation.

5. Conclusions

This study compared two fungus-growing termite mounds from a granulometric and a micromorphological perspective. It aimed at identifying modifications brought to the soil by fungus-growing termites in a semiarid subtropical region of northern Botswana in order to assess the impact fungus-growing termites have on these environments. This research was performed on two distinct substrates, one fine, one coarse, offering the opportunity to compare two different and contrasting grain-size settings. Important grain-size distribution changes were observed when comparing both termitaria and their respective control soils. In the case of the termitarium built on coarse grains, a depletion is observed in the sand fraction (180 μm) with an increase in the fine silt fraction (7 μm). The termitarium built on fine grain sediments displays an opposite trend, with a depletion in the fine silt fraction and an enrichment in the fine sand fraction. Important changes attributed to fungus-growing termites have also been observed in terms of micromorphological patterns, the most striking one being the banded arrangement of the microstructure found inside the fine grain mound, a basic distribution not observed in the corresponding control soil. This study showed that fungus-growing termites can reach a granulometric target for a given composition range. Subordinately, termites are capable of recognizing different grain sizes, and actively look for particles of the right size to be inserted into the mound material to balance its properties. It seems that fungus-growing termites can (i) adapt to any kind of parent material to build their mounds, (ii) and enrich or deplete the parent soil to meet their texture requirements in terms of mound stability and appropriate settings to insure the success of the colony. It is important to mention that modifications in texture and patterns resulting from termite activity in these subtropical regions may remain for a considerable time, impacting the grain-size distributions of the surficial sediments. Therefore, fungus-growing termites are not only ecosystem engineers but also geological agents.

Appendix A. Supplementary data

Supplementary data to this article can be found online at https://doi.org/10.1016/j.jaridenv.2021.104566.

References

Aanen, D.K., Eggleton, P., 2005. Fungus-growing termites originated in African rainforest. Curr. Biol. 15, 851–855.

Abe, S.S., Yamamoto, S., Wakatsuki, T., 2009. Soil-particle selection by the mound-building termite *Macrotermes bellicosus* on a sandy loam soil catena in a Nigerian tropical savanna. J. Trop. Ecol. 25, 449–452.

Adatte, T., Stinnesbeck, W., Keller, G., 1996. Lithostratigraphic and Mineralogic Correlations of Near K/T Boundary Sediments in North-eastern Mexico: Implications for Origin and Nature of Deposition, vol. 307. Geological Society of America Special Paper, pp. 211–226.

Baillieul, T.A., 1975. A reconnaissance survey of the cover sands in the Republic of Botswana. J. Sediment. Petrol. 45, 494–503.

Beck, H.E., Zimmermann, N.E., McVicar, T.R., Vergopolan, N., Berg, A., Wood, E.F., 2018. Present and future Köppen-Geiger climate classification maps at 1-km resolution. Sci. Data 5, 180214.

Bull, P.A., 1981. Environmental reconstruction by electron microscopy. Prog. Phys. Geogr. 5, 368–397.

Burrough, S.L., Thomas, D.S.G., 2008. Late quaternary lake-level fluctuations in the mababe depression: middle kalahari paleolakes and the role of Zambezi inflows. Quat. Res. 69, 388–403.

Cholnoky, B.J., 1966. Die Diatomeen im Unterlaufe des Okawango-Flusses. Beih. Nova Hedwigia 21, 1–102.

Cook, H.J., 1980. Landform evolution in the context of climatic change and neo-tectonism in the Middle Kalahari of north-central Botswana. Trans. Inst. Br. Geogr. 5, 80–99.

Crouvi, O., Amit, R., Enzel, Y., Gillespie, A.R., 2010. Active sand seas and the formation of desert loess. Quat. Sci. Rev. 29, 2087–2098.

Darlington, J.P.E.C., Dransfield, R.D., 1987. Size relationships in nest populations and mound parameters in the termite *Macrotermes michaelseni* in Kenya. Insectes Soc. 33, 165–180.

Davies, A.B., Baldeck, C.A., Asner, G.P., 2016. Termite mounds alter the spatial distribution of African savanna tree species. J. Biogeogr. 43, 301–313.

Dietze, E., Hartmann, K., Diekmann, B., IJmker, J.I., Lehmkuhl, F., Opitz, S., Stauch, S.G., Wünnemann, B., Borchers, A., 2012. An end-member algorithm for deciphering modern detrital processes from lake sediments of Lake Donggi Cona, NE Tibetan Plateau, China. Sediment. Geol. 243–244, 169–180.

Erens, H., Mujinya, B.B., Mees, F., Baert, G., Boeckx, P., Malaisse, F., Van Ranst, E., 2015. The origin and implications of variations in soil-related properties within *Macrotermes falciger* mounds. Geoderma 249–250, 40–50.

Francis, M.L., Ellis, F., Lambrechts, J.J.N., Poch, R.M., 2012. A micromorphological view through a Namaqualand termitaria (Heuweltjie, a Mima-Like mound). Catena 100, 57–73.

Gamrod, J.L., 2009. Paleolimnological Records of Environmental Change Preserved in Paleo-Lake Mababe, Northwest Botswana. Bachelor of Science in Geology. Southern Methodist University, Dallas, TX.

Grove, A.T., 1969. Landforms and climatic change in the kalahari and ngamiland. Geogr. J. 135, 191–212.

Humphries, M.S., Mc Carthy, T.S., 2014. The role of airborne dust in the growth of tree islands in the Okavango. Geomorphology 206, 307–317.

Jones, J.A., 1990. Termites, soil fertility and carbon cycling in dry tropical Africa: a hypothesis. J. Trop. Ecol. 6, 291–305.

Jones, B.T.B., 2002. Chobe Enclave, Botswana. Lessons Learnt from a CBNRM Project 1993-2002. CBNRM Support Programme Occasional Paper No.7. IUCN/SNV CBNRM Support Programme.

Jouquet, P., Lepage, M., Velde, B., 2002. Termite soil preferences and particle selections: strategies related to ecological requirements. Insectes Sociaux 49, 1–7.

Jouquet, P., Bottinelli, N., Shanbhag, R.R., Bourguignon, T., Traoré, S., Abbas Abbasi, S., 2016. The neglected soil engineers of tropical soils. Soil Sci. 181, 157–165.

Jouquet, P., Caner, L., Bottinelli, N., Chaudhari, E., Cheik, S., Riotte, J., 2017. Where do South-Indian termite mound soils come from? Appl. Soil Ecol. 117–118, 190–195.

Kinabo, B.D., Hogan, J.P., Atekwana, E.A., Abdelsalam, M.G., Modisi, M.P., 2008. Fault growth and propagation during incipient continent rifting: insights from a combined aeromagnetic and Shuttle Radar Topography Mission digital elevation model investigation of the Okavango Rift Zone, northern Botswana. Tectonics 27. TC3013.

Korb, J., Linsenmair, K.E., 1998. The effects of temperature on the architecture and distribution of Macrotermes bellicosus (Isoptera, Macrotermitinae) mounds in different habitats in a West African Guinea savanna. Insectes Soc. 45, 51–65.

Lancaster, N., 1981. Grain size characteristics of namib desert linear dunes. Sedimentology 28, 115–122.

Lancaster, N., 1986. Grain size characteristics of linear dunes in the southwestern Kalahari. J. Sediment. Petrol. 56, 395–400.

Landman, W.A., Mason, S.J., Tyson, P.D., 2001. Retro-active skill of multi-tiered forecasts of summer rainfall over southern Africa. Int. J. Climatol. 21, 1–19.

McCarthy, T.S., Metcalfe, J., 1990. Chemical sedimentation in the semi-arid environment of the Okavango Delta, Botswana. Chem. Geol. 89, 157–178.

Mermut, A.R., Arshad, M.A., St Arnaud, R.J., 1984. Micropedological study of termite mounds of three species of Macrotermes in Kenya. Soil Sci. Soc. Am. J. 48, 613–620.

Michalopoulos, P., Aller, R.C., Reeder, R.J., 2000. Conversion of diatoms to clays during early diagenesis in tropical, continental shelf muds. Geology 28, 1095–1098.

Modisi, M.P., Atekwana, E.A., Kampunzu, A.B., Ngwisanyi, T.H., 2000. Rift kinematics during the incipient stages of continental extension: evidence from the nascent Okavango rift basin, northwest Botswana. Geology 28 (10), 939–942.

Ocko, S.A., Heyde, A., Mahadevan, L., 2019. Morphogenesis of termite mounds. Proc. Natl. Acad. Sci. Unit. States Am. 116 (9), 3379–3384.

Pansu, M., Gautheyrou, J., Aventurier, A., Feller, C., Bottner, P., 2003. L'analyse du sol : minéralogie, organique et minérale. Institut de Recherche pour le Développement, Springer, ISBN 2-287-59774-3, p. 1012.

Pomeroy, D.E., 1978. The abundance of large termite mounds in Uganda in relation to their environment. J. Appl. Ecol. 15, 51–63.

Prospero, J.M., Ginoux, P., Torres, O., 2002. Environmental characterization of global sources of atmospheric soil dust identified with the nimbus 7 total ozone mapping spectrometer (TOMS) absorbing aerosol product. Rev. Geophys. 40, 1012.

Ringrose, S., Huntsman-Mapila, P., Downey, W., Coetzee, S., Fey, M., Vanderpost, C., Vink, B., Kemosidile, T., Kolokose, D., 2008. Diagenesis in Okavango fan and adjacent dune deposits with implications for the record of palaeo-environmental change in Makgadikgadi–Okavango–Zambezi basin, northern Botswana. Geomorphology 101, 544–557.

Romanens, R., Pellacani, F., Mainga, A., Fynn, R., Vittoz, P., Verrecchia, E.P., 2019. Soil diversity and major soil process in the kalahari basin, Botswana. Geoderma Regional 19 e00236.

Rowley, M.C., Grand, S., Verrecchia, E.P., 2018. Calcium-mediated stabilisation of soil organic carbon. Biogeochemistry 137, 27–49.

Stoops, G., 2003. Guidelines for Analysis and Description of Soil and Regolith Thin Sections. Soil Science society of America, Madison, WI, p. 184.

Stoops, G., Marcelino, V., Mees, F., 2018. Interpretation of Micromorphological Features of Soils and Regoliths, second ed. Elsevier, Amsterdam, p. 982.

Thomas, D.S.G., Shaw, P.A., 1991. The Kalahari Environment. Cambridge University Press, Cambridge, UK, p. 284.

Turner, J.S., 2006. Termites as mediators of the water economy of arid savanna ecosystems. In: D'Odorico, P., Porporato, A. (Eds.), Dryland Ecohydrology, pp. 303–313.

Tyson, P.D., Garstang, M., Swap, R., Kållberg, P., Edwards, M., 1996. An air transport climatology for subtropical southern Africa. Int. J. Climatol. 16, 265–291.

Vittoz, P., Pellacani, F., Romanens, R., Mainga, A., Verrecchia, E.P., Fynn, R.W.S., 2020. Plant community diversity in the Chobe Enclave, Botswana: insights for functional habitat heterogeneity for herbivores. Koedoe 62, a1604.

Wang, L., D'Odorico, P.D., Ringrose, S., Coetzee, S., Macko, S.A., 2007. Biogeochemistry of kalahari sands. J. Arid Environ. 71, 259–279.

Watson, J.P., 1969. Water movement in two termite mounds in Rhodesia. J. Ecol. 57, 441.

Watson, J.P., 1975. The composition of termite (Macrotermes spp.) mounds on soil derived from basic rock in three rainfall zones of Rhodesia. Geoderma 14, 147–158.

Watson, A., 1986. Grain size variations on a longitudinal dune and a barchan dune. Sediment. Geol. 46, 49–66.

West, W.F., 1970. The bulawayo symposium papers, No2: termite prospecting. Chamb. Mines J. 30, 32–35.